



UNIVERSITY OF LEEDS

This is a repository copy of *Characterisation of fractured carbonate aquifers using ambient borehole dilution tests*.

White Rose Research Online URL for this paper:  
<https://eprints.whiterose.ac.uk/162854/>

Version: Accepted Version

---

**Article:**

Agbotui, PY, West, LJ [orcid.org/0000-0002-3441-0433](https://orcid.org/0000-0002-3441-0433) and Bottrell, SH (2020)  
Characterisation of fractured carbonate aquifers using ambient borehole dilution tests.  
Journal of Hydrology, 589. 125191. ISSN 0022-1694

<https://doi.org/10.1016/j.jhydrol.2020.125191>

---

© 2020 Elsevier. All rights reserved. This manuscript version is made available under the CC-BY-NC-ND 4.0 license <http://creativecommons.org/licenses/by-nc-nd/4.0/>.

**Reuse**

This article is distributed under the terms of the Creative Commons Attribution-NonCommercial-NoDerivs (CC BY-NC-ND) licence. This licence only allows you to download this work and share it with others as long as you credit the authors, but you can't change the article in any way or use it commercially. More information and the full terms of the licence here: <https://creativecommons.org/licenses/>

**Takedown**

If you consider content in White Rose Research Online to be in breach of UK law, please notify us by emailing [eprints@whiterose.ac.uk](mailto:eprints@whiterose.ac.uk) including the URL of the record and the reason for the withdrawal request.



[eprints@whiterose.ac.uk](mailto:eprints@whiterose.ac.uk)  
<https://eprints.whiterose.ac.uk/>

1 TITLE: **Characterisation of fractured carbonate aquifers using ambient borehole dilution tests**

2 Prodeo Yao Agbotui<sup>1,2</sup>, Landis Jared West<sup>1</sup>, Simon Henry Bottrell<sup>1</sup>

3 <sup>1</sup> School of Earth and Environment, University of Leeds, Woodhouse Lane, Leeds, West Yorkshire, LS2

4 9JT, United Kingdom. Author email addresses: [ee08pya@leeds.ac.uk](mailto:ee08pya@leeds.ac.uk); [l.j.west@leeds.ac.uk](mailto:l.j.west@leeds.ac.uk);

5 [s.bottrell@leeds.ac.uk](mailto:s.bottrell@leeds.ac.uk)

6 Corresponding author: Landis Jared West, email address [l.j.west@leeds.ac.uk](mailto:l.j.west@leeds.ac.uk), correspondence

7 address: School of Earth and Environment, University of Leeds, Woodhouse Lane, Leeds, West

8 Yorkshire, LS2 9JT, United Kingdom

9

---

<sup>2</sup> Permanent Address: Department of Civil Engineering, Accra Technical University, Accra Central, Ghana, West Africa

## 10 **Abstract**

11 Fractured carbonate aquifers derive their transmissivity essentially from a well-developed network of  
12 solutionally-enhanced fractures and conduits that can lead to high groundwater velocities and high  
13 vulnerability to contamination of water quality. Characterisation of the variation of hydraulic  
14 properties with depth is important for delineating source protection areas, characterising  
15 contaminant fate and transport, determination of the effectiveness of aquifer remediation, and  
16 parameter estimation for models. In this work, ambient open borehole uniform and point injection  
17 dilution tests were conducted on observation boreholes in the unconfined Cretaceous Chalk aquifer  
18 of East Yorkshire, UK, and interpreted in conjunction with other data via the implementation of a new  
19 work flow. This resulted in the characterisation of flow in these boreholes and the inference of  
20 properties such as groundwater flow patterns and velocities in the surrounding aquifer formation. Our  
21 workflow allowed sections of open boreholes showing horizontal versus vertical flow to be  
22 distinguished, and the magnitude of such flows and exchanges with the aquifer to be determined.  
23 Flow within boreholes were then used to characterise: i) presence and direction of vertical hydraulic  
24 gradients; ii) nature and depth distribution of flowing features; iii) depth interval porosity and  
25 permeability estimation of the flowing features from overall borehole transmissivity and geophysical  
26 image or caliper logs; iv) groundwater velocity estimation in the surrounding aquifer. Discrete flowing  
27 features were distributed across the range of depths sampled by the observation boreholes (typically  
28 up to 45 to 60 mbgl), but the majority were located in the zone of water table fluctuation marked by  
29 solutionally enlarged flow features. Quantitative interpretation of both uniform injection (tracer  
30 distributed throughout the open borehole section) and point injection (slug of tracer introduced at  
31 targeted depth) yielded vertical velocities within the borehole water column in broad agreement with  
32 those measured by flow logging. Depth specific fracture kinematic porosities inferred from the  
33 ambient dilution data combined with long-interval pump test and geophysical log data ranged  
34 between  $3.7 \times 10^{-4}$  –  $4.1 \times 10^{-3}$  with an average of  $2.1 \times 10^{-3}$ ; these values were in excellent agreement  
35 with those from other methods applied to the same aquifer such as larger scale pumping tests. A new

36 approach to estimation of groundwater velocities from the dilution test data using externally  
37 measured hydraulic gradients gave inferred horizontal groundwater velocities ranging between 60 –  
38 850 m/day, in full agreement with those from previously conducted borehole-to-borehole tracer tests.  
39 These results confirm that the studied aquifer is karstic, with rapid preferential pathways which have  
40 implication for flow and transport modelling, and pollution vulnerability. Our study results indicate  
41 that ambient single-borehole dilution approaches can provide an inexpensive and reliable approach  
42 for the characterisation of fractured and karstic aquifers.

43 **Keywords:** Fractured aquifer, borehole dilution, tracer tests, wellhead protection, carbonate, aquifer  
44 vulnerability.

## 45 **1. Introduction**

46 Preferential flowpaths and vertical head gradients are pervasive in fractured rock aquifers (Singhal  
47 and Gupta, 1999; Cook, 2003). Knowledge of fracture and conduit connectivity and vertical hydraulic  
48 gradients are important for aquifer characterisation and developments such as: the design and  
49 development of abstraction boreholes, targeted horizon sampling for chemical characterisation (Moir  
50 et al., 2014; McMillan et al., 2014), groundwater flow interpretation and modelling (Saines, 1981;  
51 Brassington, 1992; Dalton et al., 2006; Weight, 2008) and effective design of remediation schemes.  
52 Methods for characterising preferential flowpaths in fractured aquifers can be classified as catchment  
53 scale and single borehole methods (Singhal and Gupta, 1999; Cook, 2003). Catchment scale tests  
54 include stream sink point-to-spring and ambient borehole-to-borehole tracer tests (Cook, 2003;  
55 Bottrell et al., 2010). These give direct measurement of groundwater velocity and fracture  
56 connectivity. However, catchment scale tracer tests are expensive and difficult to set up. Cheaper  
57 single-borehole characterisation approaches include core sampling (Shuter and Teasdale, 1989),  
58 conventional geophysical logging (Keys, 1990), caliper logging (Paillet and Pedler, 1996), borehole  
59 CCTV (Zemanek et al., 1970; Paillet, 1991), packer testing (Quinn et al., 2011), flow logging (Molz et  
60 al., 1989; Parker et al., 2010), and single borehole dilution testing (Tsang et al., 1990; Tsang and

61 Doughty, 2003; West and Odling, 2007; Maurice et al., 2010; Parker et al., 2010), amongst others. Core  
62 logging and sampling can be problematic for carbonate aquifers where flow is dominantly in fractures  
63 and conduits, due to inability to preserve fracture properties in the recovered core. Conventional  
64 borehole geophysical techniques use the borehole wall or fluid properties such as neutron, gamma  
65 and resistivity logging, and caliper logs to measure borehole wall enlargements which often coincide  
66 with fractures (which may or may not be flowing features). Borehole CCTV and image logs provide a  
67 view of borehole wall properties by showing fractures, but not all fractures detected are flowing  
68 features. Borehole fluid flow logging under pumped and or ambient conditions and/or packer tests  
69 are typically used to evaluate hydraulic conductivity and flow variation with depth (Day-Lewis et al.,  
70 2011; Parker et al., 2010; Medici et al., 2018; Quinn et al., 2011). In impeller flow logging, increase or  
71 decrease in borehole vertical flows within a logged interval is used to infer inflow or outflow to the  
72 aquifer respectively. However, impeller flow logging is expensive, and is insensitive to small ambient  
73 flows (Pitrak et al., 2007). Impeller flow logging is also not able to detect horizontal crossflows in  
74 boreholes (Paillet and Pedler, 1996; Maurice et al., 2010). In packer testing, sealing in open boreholes  
75 in fractured formations often presents difficulties because of wall irregularities, and skin effects may  
76 cause errors in hydraulic conductivity estimation. Also, hydraulic conductivity estimation requires  
77 assumptions about the shape of the flow field which are based on granular aquifers and nearly always  
78 wrong in fracture flow systems (Boulding, 1993; Singhal and Gupta, 1999). Furthermore, packer tests  
79 sample only a small volume of the aquifer near the borehole wall except where they are conducted  
80 on intervals with highly transmissive fractures (Paillet et al., 2012). In contrast, single borehole  
81 dilution testing characterises hydraulic properties by interpreting the tracer concentration profile  
82 development resulting from inflowing formation water. Compared to other borehole characterisation  
83 techniques, single borehole dilution is not only relatively easier to set up, but is also highly sensitive  
84 to low ambient flows in boreholes. It can also detect crossflows. Improved interpretation is possible  
85 when combined with data from image and caliper logs (Kobr, 2003; Maurice et al., 2010). Tsang et al.  
86 (1990), Kobr (2003), Doughty et al. (2005), Doughty et al. (2008), Datel et al. (2009) and Maldaner et

87 al. (2018) found good agreement between single borehole dilution interpretations and those from  
88 other single borehole characterisation methods like core logging, packer and slug testing, flow logging  
89 and conventional geophysical logging.

90 Extending single borehole dilution test interpretation to the catchment scale would reduce  
91 investigation cost, and remove the difficulty and uncertainty associated with the performance of  
92 borehole-to-borehole tracer tests. However, there are few published examples where ambient single  
93 borehole tests are validated by catchment scale measurements. Novakowski et al. (2006) for instance  
94 used ambient borehole-to-borehole tracer tests to validate single borehole dilution tests in limestone  
95 and dolostone aquifers in Ontario, Canada. In that work the single-borehole method used was more  
96 expensive than that used in our study described in this paper, in that packers and standpipes were  
97 installed in the boreholes. However, their study successfully showed that single borehole dilution  
98 tested fractures that were conductive at the catchment scale had comparable fracture hydraulic  
99 gradients to the regional hydraulic gradient and also had same order of magnitude fracture velocities  
100 to groundwater velocities from natural borehole-to-borehole tracer tests. In contrast, hydraulic  
101 gradients and fracture velocities of local fractures were dissimilar to that from borehole-to-borehole  
102 tracer tests.

103 In this work we develop the ambient single borehole dilution tests approach and validate the results  
104 against other methods (single borehole optical, caliper logging and borehole flow logging and  
105 borehole-to-borehole tracer testing). We present a new workflow which involves determination of  
106 flowing horizons and dominant flow mechanisms from single-borehole dilution data, followed by  
107 application of quantitative analysis to both uniform injection and point injection test results. The new  
108 workflow is applied to a series of ambient single borehole dilution tests performed in four boreholes  
109 in the Kilham Catchment of the East Yorkshire Chalk Aquifer, United Kingdom: a fractured carbonate  
110 aquifer. Via the implementation of a new methodology and decision process, boreholes dominated  
111 by either horizontal or vertical flows were identified. In cases where vertical flow in the borehole water

112 column dominated, vertical borehole fluid velocities and tracer mass losses were quantified. In cases  
113 where horizontal flows dominated, groundwater velocities in the surrounding aquifer were found  
114 combined with the regional hydraulic gradient. In each case, the single-borehole test data was used  
115 to inform a conceptual model of flow in the aquifer at the borehole-test scale. Borehole-test scale  
116 groundwater velocities were then validated against those inferred from borehole-to-borehole tracer  
117 tests.

## 118 **2. Theoretical development and analytical concepts**

### 119 *2.1 Single borehole dilution tests and analytical methods*

120 Single borehole dilution testing is a technique used to characterise borehole hydraulic properties and  
121 flow variation with depth in open boreholes in aquifer formations (i.e.  $K > 10^{-6}$  m/s, Pitrak et al., 2007)  
122 often via monitoring specific electrical conductance (SEC) contrasts between aquifer formation fluid  
123 and borehole fluid column following the introduction of a tracer in the borehole (Tsang et al., 1990;  
124 Pedler et al., 1990; Pedler et al., 1992; Kobr, 2003; West and Odling, 2007; Maurice et al., 2010; Paillet  
125 et al., 2012). Single borehole dilution testing can be undertaken under pumped (eg. Brainerd and  
126 Robbins, 2004; Pedler et al., 1992; Tsang et al., 1990; West and Odling, 2007) or ambient (eg. Drost et  
127 al., 1968; Lewis et al., 1966; Maurice et al., 2010) conditions, using either uniform and point injection  
128 approaches. In uniform injection, the entire section of the borehole that is open to the aquifer is  
129 injected with a tracer. Horizontal flow across the borehole is indicated by proportional tracer dilution  
130 with time, whereas vertical flow in the borehole is depicted by movement of the boundary of the  
131 tracer and inflowing formation water along the vertical axis of the borehole. In point injection, a tracer  
132 slug is injected at a targeted depth, and the tracer slug is monitored for vertical movement and mass  
133 loss along the axis of the borehole.

134 The single borehole dilution method has advantages as compared to other borehole investigation  
135 techniques. The method is sensitive to very low ambient flows that cannot be resolved by impeller  
136 flowmeters (Tsang et al., 1990; West and Odling, 2007) and can also detect crossflows under both

137 ambient and pumped conditions (Doughty and Tsang, 2005; West and Odling, 2007; Maurice et al.,  
 138 2010). It is also less expensive in relation to packer tests (Tsang et al., 1990; Tsang and Doughty, 2003;  
 139 West and Odling, 2007) and flowmeter logging (Tsang et al., 1990; Pedler et al., 1990). However,  
 140 correct interpretation of single-borehole test data requires that tracer dispersion within the borehole  
 141 water column is distinguished from the effects of tracer dilution by inflows from flowing features and  
 142 mass loss through outflows (Brainerd and Robbins, 2004; West and Odling, 2007). Secondly, borehole  
 143 dilution tests are not suitable for characterising non-aquifers because processes like diffusion, density  
 144 driven flows and probe signal artefacts can dominate over those modelled by tracer dilution ( Ward  
 145 et al., 1998).

146 Common tracers used for the single borehole dilution testing include NaCl (West and Odling, 2007;  
 147 Maurice et al., 2010; Moir et al., 2014), deionised water (Pedler et al., 1990; Tsang et al., 1990),  
 148 fluorescein (Lewis et al., 1966) and food dyes (Pitrak et al., 2007). NaCl was chosen as a tracer for this  
 149 work because it is inexpensive, readily available, easy and safe to handle and non-toxic to humans  
 150 and the environment and can be monitored via SEC signature (Ward et al., 1998). Note that in very  
 151 rapid flow conditions, EC measurements may become inaccurate and other tracers such as  
 152 fluorescein or food dyes may be preferable (Pitrak et al., 2007). Also NaCl concentration > 120 g/L  
 153 can cause density driven flows ( Ward et al., 1998).

154 Generally, the single borehole dilution test is analysed and interpreted from the tracer concentration  
 155 difference between initial injection time and subsequent times as a result of influx and mixing with  
 156 fresh formation water diluting the tracer. The analytical techniques for analysing single borehole  
 157 dilution tests are based on mass conservation theories and the solution to solute transport models  
 158 such as the 1-dimensional advection dispersion equation (ADE). The ADE models the rate of change  
 159 of tracer concentration in the borehole water column with respect to time (West and Odling, 2007):

$$\frac{\partial C(z, t)}{\partial t} = -\frac{\partial(Cu(z, t))}{\partial z} + \frac{\partial}{\partial z} \left[ \alpha_B u(z, t) \frac{\partial C}{\partial z} \right] - \frac{CQ_o(z, t)}{\pi r_w^2} \quad (1)$$



160 where  $C(z,t)$  is the concentration at time  $t$  after tracer injection at elevation  $z$ ,  $u(z,t)$  is vertical fluid  
161 velocity in the borehole,  $Q_o(z,t)$  is the volumetric inflow rate of formation water of zero tracer  
162 concentration per unit depth of borehole per unit time,  $r_w$  is the borehole radius, and  $\alpha_B$  is the  
163 coefficient of dispersivity in the flow direction (i.e. vertical). The first term on the right of Equation (1)  
164 represents vertical advective effect of the flow in the borehole. The second term describes vertical  
165 'Fickian' dispersion of tracer. The last term represents dilution effect of inflowing formation water and  
166 loss of tracer from outflow. The assumptions are thus that dispersion within the borehole water  
167 column is Fickian, i.e. the solute distribution is Gaussian; borehole diameter is small compared to the  
168 length which allows full mixing between the inflowing and the borehole water at each depth interval;  
169 and density-driven effects are negligible in the borehole. Mass conservation implies that both water  
170 discharge and solute mass entering a fracture or set of fractures is equal to the difference in vertical  
171 flow and mass flux in the borehole above and below these fractures (Tsang et al., 1990; Brainerd and  
172 Robbins, 2004; Doughty and Tsang, 2005).

173 Methods for analysing single borehole dilution test data include: the 'signature' method, analytical,  
174 modelling/curve fitting and combined techniques. The signature approaches give a qualitative  
175 interpretation and understanding of flow processes in boreholes from the analyses of various features  
176 created by inflow, outflow, crossflow and vertical flow on temporal tracer profiles (Doughty and Tsang,  
177 2005; Maurice et al.,2010). Signature approaches are simple to use but are subjective and sometimes  
178 produce non-unique interpretation (Doughty and Tsang, 2005; Maurice et al.,2010). Quantitative  
179 analytical methods use the mass balance of solute to infer flow properties for pumped-borehole  
180 dilution tests (Tsang et al., 1990), and for the specific case of horizontal crossflow in ambient  
181 conditions (Drost et al., 1968; Lewis et al., 1966; Ward et al., 1998; Pitrak et al., 2007). The analytical  
182 techniques provide useful information when used in conjunction with other types of complementary  
183 analyses, but on their own are overly simplistic for real world problems (Doughty and Tsang, 2005;

184 Ward et al., 1998). These modelling approaches fit the field SEC profile to, for example, the 1-D ADE  
185 model (Doughty and Tsang, 2005; West and Odling, 2007) by specifying flowing feature elevations and  
186 varying the discharge and solute concentration at the fracture (BORE codes, I & II in Tsang et al., 1990),  
187 or varying flow velocity and vertical dispersivity in the borehole until there is a good fit between the  
188 field data and the ADE (West and Odling, 2007). Combined approaches model the tracer profile  
189 development using both the signature and analytical techniques to constrain flow characteristics in  
190 the borehole (Doughty and Tsang, 2005; Maurice et al., 2010). They are simple to use, more efficient  
191 and require less time and effort, and provide a better constraint on flow in boreholes (Doughty and  
192 Tsang, 2005; Moir et al., 2014). In this work, we focus on the combined approach for analysing single  
193 borehole dilution tests in ambient flow conditions.

194 Analysis approaches for ambient-flow open borehole dilution tests in a fractured aquifer like the Chalk  
195 assume that flow occurs via discrete horizons (Singhal and Gupta, 1999; Cook, 2003). Due to hydraulic  
196 head differences between the layers, recharge and discharge areas of the aquifer are often dominated  
197 by vertical flows. In transition zones between recharge and discharge areas, where head gradients  
198 between flowing features are small, horizontal crossflows often dominate. In some areas, a  
199 combination of vertical and horizontal flows can be present within a single borehole water column  
200 (Toth, 1962; Freeze and Witherspoon, 1968; Brassington, 1992; Toth, 2009; Liang et al., 2010). Single  
201 borehole tracer signatures produced from horizontal crossflow versus vertical flows are presented in  
202 detail in Doughty and Tsang (2005) and Maurice et al. (2010).

203 For the case of borehole sections dominated by horizontal crossflow, the horizontal specific discharge  
204 can be found assuming that: the concentration across the borehole water column is uniform (ie well  
205 mixed), there are no vertical flows and that flow is steady-state; then the first and second terms of  
206 equation (1) are negligible. Integrating (1) and using the boundary conditions of  $C$  from  $C_o$  to  $C_i$ , and  
207 time from 0 to time,  $t$  and re-arranging yields:

$$\ln C_t = -\left(\frac{2q_w}{\pi r_w}\right)t + \ln C_0 \quad (2) \quad 208$$

209

$$\text{where } q_w = \alpha q_f \quad (3),$$

210

211 where  $q_w$  is the horizontal specific discharge or Darcian flux through the borehole interval,  $q_f$  is the  
 212 formation specific discharge,  $\alpha$  is the dimensionless flow constriction factor that accounts for flow  
 213 convergence and distortion from the formation into the open section of the borehole (Drost et al.,  
 214 1968; Gustafsson and Anderson, 1991), defined by the ratio of the aquifer width contributing to flow  
 215 to the borehole to the borehole diameter, and  $C_t$  is concentration at any time  $t$  after injection of  
 216 tracer.

217 Plotting the natural logarithm of concentration versus time at depth of interest produces a linear  
 218 response (hereon referred to as the Pitrak et al. (2007) method), with the slope,  $m$  of the tracer decay  
 219 line proportional to  $q_w$  i.e.:

$$q_w = \frac{m\pi r_w}{2} \quad (4).$$

220

221 Finding  $q_f$  using eqn (2) and dividing by  $\phi_e$ , the fracture kinematic porosity, yields the average linear  
 222 velocity of groundwater in the formation  $v_{fh}$ :

$$v_{fh} = \frac{q_f}{\phi_e} = \frac{q_w}{\alpha\phi_e} = \frac{m\pi r_w}{2\phi_e\alpha} \quad (5).$$

223

224 Constraining the values of  $\alpha$  and  $\phi_e$  are the main difficulty in using equation (5). The flowing fracture  
 225 porosity  $\phi_e$  can be estimated from hydraulic tests, and the number of flowing fractures intersecting  
 226 the borehole interval from geophysical logging, by assuming the cubic law for parallel fractures, see

227 section 2.2 below (Novakowski et al., 2006; Quinn et al., 2011; Maldaner et al., 2018; Medici et al.,  
228 2019).

229 For the case of borehole sections with dominant ambient vertical flows, equation (2) is not applicable  
230 because of vertical flow effects (Drost et al., 1968; Ward et al., 1998; Pitrak et al., 2007; Piccinini et al.,  
231 2016). In that case, tracer will travel vertically along the borehole with dilution and/or mass loss from  
232 inflow and outflow/crossflow features respectively (Maurice et al., 2010). The mass of solute under  
233 any concentration profile is given (Doughty and Tsang, 2005) as:

$$M = \int [C(z) - C_0] \pi r_{wa}^2 dz \quad (6)$$

234

235 In equation (6),  $r_{wa}$  is the average borehole radius from caliper log. Applying equation (6) to ambient  
236 flow uniform injection test data is difficult due to possible dispersion and interference of flowing  
237 feature signatures. However, for the case of point injection of a tracer slug at a discrete depth,  
238 comparison of sequential profile  $M$  values indicates where mass is conserved (no outflow) versus lost  
239 (outflow), and comparison of masses above and below flowing features indicates the extent of tracer  
240 mass lost. Furthermore, sequential profile centroid positions can be used to estimate velocity of  
241 vertical flow,  $u$ . Using the profile velocities and borehole radius from caliper logs where available,  
242 vertical discharge  $Q_v$  is computed (Kobr, 2003) as:

$$Q_v = \pi r_{wa}^2 u \quad (7)$$

243

244 Using the mass integrals under the profiles and the differences between  $Q_v$  for adjacent borehole  
245 sections, the magnitude of borehole inflows and outflows associated with specific flowing features  
246 or intervals are constrained. This approach informs the development of conceptual models of flow  
247 for each tested borehole.

248 2.2 The parallel plate model (cubic law)

249 In a borehole intersected by fractures, flowing fracture aperture,  $a_f$  can be found from the fracture  
250 transmissivity  $T_f$  using the parallel plate model, also called the cubic law (Snow, 1969; Witherspoon  
251 et al., 1980; Qian et al., 2011):

$$252 \quad a_f = \sqrt[3]{\frac{12\nu T_f}{g}} \quad (8)$$

253 where  $\nu$  and  $g$  are the kinematic viscosity of water ( $1.307 \times 10^{-6} \text{ m}^2\text{s}^{-1}$ ) and acceleration due to  
254 gravity, ( $9.81 \text{ ms}^{-2}$ ) respectively.  $T_f$  is the single aperture transmissivity, and is defined as:

$$255 \quad T_f = \frac{T_i}{N_i} \quad (9)$$

256 where  $T_i$  is the transmissivity of the borehole interval (i.e. vertical section of borehole) and  $N_i$  is the  
257 number of flowing features intersecting that interval e.g. identified from geophysical and core logging.

258 The effective fracture porosity  $\phi_e$  for the formation intersected by the interval with length  $L$  can  
259 thus be determined as:

$$260 \quad \phi_e = \frac{N_i a_f}{L} \quad (10)$$

261 As an alternative to equation (5), the average horizontal velocity of groundwater in the formation  
262 intersected by the borehole interval can also be found using the regional hydraulic gradient  $i_f$   
263 together with the fracture aperture  $a_f$

$$264 \quad v_{fh} = k_f \cdot i_f = \frac{(a_f)^2 g}{12\nu} i_f \quad (11)$$

265 where  $k_f$  and  $i_f$  are the fracture hydraulic conductivity and hydraulic gradient in the formation  
266 surrounding the borehole respectively. The assumptions for using equations (8) to (11) to find the  
267 average horizontal groundwater velocity in the formation are that the flowing features intersecting

268 the interval are horizontal or shallowly dipping fractures with equal transmissivity and hence hydraulic  
269 aperture implying that:

$$270 \quad k_f = \frac{T_f}{a_f} \quad (12)$$

271 Groundwater velocities have been derived from single borehole tests undertaken by previous workers  
272 who either used straddle packers (Novakowski et al., 1995; Xu et al., 1997; van Tonder et al., 2002;  
273 Novakowski et al., 2006; Akoachere and Van Tonder, 2009; Maldaner et al., 2018) or depth specific  
274 piezometers (Piccinini et al., 2016; Medici et al., 2019) to isolate borehole sections. In this paper, we  
275 combine this approach with borehole dilution tests to determine the variation in effective fracture  
276 porosity with depth for long open borehole sections. We compare groundwater velocities derived  
277 from single borehole tests with those from borehole-to-borehole tracer tests in order to validate the  
278 method.

### 279 **3. Study area**

280 The aquifer on which the study area is located is the unconfined area of the Cretaceous Chalk aquifer  
281 in East Yorkshire, NE England, UK (Figure 1). In the United Kingdom (UK), the Chalk is the most  
282 important aquifer, providing about 60% of public water supply contributed by groundwater (Allen et  
283 al., 1997; Downing, 1998; Knapp, 2005). In East Yorkshire, the Chalk is the main source of potable  
284 water supply for domestic and industrial supplies (Edmunds et al., 2001; Smedley et al., 2004; Gale  
285 and Rutter, 2006). The Chalk also supports the ecology and the conservation Sites of Special Scientific  
286 Importance (SSSI) of the River Hull, the headwaters of which are groundwater fed (Gale and Rutter,  
287 2006). The Chalk aquifer lies uncomfortably over Jurassic Formations with the main aquifer units being  
288 the Flamborough, Burnham and Welton Formations. The bedding dips at 2° to the south-east. The  
289 Chalk aquifer derives its high transmissivity from a well-developed network of solutionally-enhanced  
290 joints, faults, bedding plane features and karst conduits or channels (Allen et al., 1997; Bloomfield,  
291 1996). The joints are steeply dipping, the majority of which are stratabound, with joint spacing ranging

292 between 0.3 – 0.5 m. Joint trace lengths range between 0.65 – 2.5 m. Bedding plane fractures are  
293 persistent laterally, making bedding plane fractures the main flowpaths for groundwater flow and  
294 contaminant transport (Bloomfield, 1996; Waters and Banks, 1997). Thin marl layers act as barriers to  
295 vertical flow, thereby concentrating flows along bedding fractures (Gale and Rutter, 2006), causing  
296 solutionally enhanced bedding-parallel flow features (widened fractures and small conduits).  
297 Although the Chalk is a dual porosity aquifer, effective storage for the aquifer is from the fracture  
298 network as the narrow pore throats ( 0.1 to 1.0  $\mu\text{m}$ ) within the Chalk matrix prevent drainage from  
299 the matrix (Price, 1987; Price et al., 2000).

300 Despite the importance of the Chalk as an aquifer, since the 1970s it has been plagued by  
301 contamination from nitrate and other agrochemicals resulting in several studies to characterise:  
302 resource assessment (Foster and Milton, 1974; Foster and Milton, 1976; Jones et al., 1993), hydraulic  
303 conductivity variation with depth (Buckley and Talbot, 1994; Bloomfield, 1996; West and Odling,  
304 2007; Parker et al., 2010; Parker et al., 2019), borehole-to-borehole tracer tests for the delineation of  
305 the source protection zone (SPZ) areas for boreholes and springs (Ward and Williams, 1995; Ward et  
306 al., 2000). The four boreholes tested here using ambient single borehole dilution tests are Field House  
307 Farm, Kilham (FHK), Little Kilham Farm (LKF), Tancred Pit (TP) and Weaverthorpe (WTP), see Figure 1.  
308 In all the boreholes, the upper parts of the boreholes are cased, with open sections below. Table 1  
309 shows the borehole details and their injection parameters. Note that the connectivity and horizontal  
310 groundwater velocities between boreholes, Henpit Hole (HPT 1 & 2) and Middledale borehole (MD) &  
311 LKF borehole were previously established using borehole-to-borehole tracer tests (see Figure 1)

312

313 **Table 1**

314 Borehole details and injection parameters of single borehole dilution tests in this study

Borehole name	UK national grid reference	Ground elevation (m AoD)	Borehole top diameter (mm)	Borehole depth (m)	Depth of open section tested (m)	Type of single borehole dilution test conducted		Mass of salt injected in tests (g)	
						Uniform	Point	Uniform	Point
Field House Kilham (FHK)	TA 071 672	68.66	208	67	24	Yes	No	450	N/A
Little Kilham Farm (LKF)	TA 046 649	39.96	202	50	32	Yes	Yes	900	75
Tancred Pit (TP)	TA 069 660	36.40	220	50	37	Yes	Yes	2500	75
Weaverthorpe (WTP)	SE 981 702	71.00	152	46	19	Yes	Yes	650	75

315

316

317



318

## 319 **4. Methods**

### 320 *4.1 Single-borehole dilution tests set up*

321 Both uniform injection (Ward et al.,1998; Pitrak et al., 2007; Maurice et al., 2010) and point  
322 emplacement (Tate et al., 1970; Kobr, 2003; Maurice et al., 2010) ambient flow single-borehole  
323 dilution tests were undertaken (Figure 2 and Table 1). Groundwater levels at the time of each test are  
324 marked on the respective figures; these were essentially similar between the different types of test.  
325 The borehole was first logged for background specific electrical conductivity (SEC) with a Solinst TLC  
326 dipper at specific depth intervals. For the uniform injection tests (Figure 2.a), NaCl solution was  
327 injected uniformly into the boreholes by filling a 25 mm diameter weighted hose ( $\{\text{NaCl}\} \leq 120 \text{ gL}^{-1}$  in  
328 hose) inserted into the borehole. The hose pipe was slowly pulled out of the borehole to produce  
329 initial uniform tracer concentration via mixing with the borehole water. Then sequential logs of SEC  
330 ( $\mu\text{S}/\text{cm}$ ) with depth were measured and converted to sodium chloride concentrations  $\{\text{NaCl}\}$  (g/L)  
331 using a calibration equation ( $\text{signal SEC} = 1714.5 \{\text{NaCl}\} + 464, R^2=0.99$ ) derived from dissolving known  
332 masses of NaCl in Chalk water and measuring the resulting SEC signal. The work flow in Figure 3 was  
333 implemented to characterise the borehole as horizontal or vertical flow dominated and for targeting  
334 depths for point injection tests. For point injection tests (Figure 2.b), target injection depths were  
335 injected with 0.5L of  $150 \text{ gL}^{-1}$  NaCl solution (i.e. 75g of NaCl) from a 1.2 m long x 70 mm diameter point  
336 injection barrel. The barrel was then dropped to the target depth and released by operating a  
337 connected Rothenberger Test pump at the ground surface. Sequential SEC measurements were made  
338 to monitor vertical migration and attenuation of the resulting sodium chloride slug within the  
339 borehole.

## 340 4.2 *Single-borehole dilution test work flow and interpretation process*

341 Figure 3 shows the workflow and decision tree for the interpretation of single-borehole dilution tests.  
342 Following signature / qualitative analyses of uniform injection tests, the method of Pitrak et al. (2007)  
343 (refer to section 2.1) was applied to the uniform injection test data to verify whether or not flow at  
344 each monitored depth interval was dominated by vertical or horizontal flow. For boreholes dominated  
345 by lateral horizontal flows, the analysis yields horizontal specific discharge versus depth. For such  
346 cases (“Yes” decision route in Figure 3), specific discharge data were combined with geophysical log  
347 and hydraulic test transmissivities and external hydraulic gradients by implementing equations 8-11  
348 (parallel plate model) to produce fracture effective porosity and horizontal fracture flow velocities  
349 versus depth. For vertical flow dominated boreholes (“No” decision route in Figure 3), point injection  
350 tests at targeted depths were analysed via plotting centroid velocity, tracer mass loss) and vertical  
351 flow rate differencing at sequential sections of the borehole. Where possible methodologies described  
352 in Doughty and Tsang (2003), Kobr (2003) and Maurice et al. (2010) were applied to find inflow and  
353 outflow fluxes into discrete fractures/intervals from the observed changes in vertical borehole flows.

## 354 **5. Results and interpretation**

### 355 **5.1 Results**

#### 356 *5.1.1 Uniform injection tests*

357 The results of uniform injection tests are shown in Figure 4. FHK borehole diameter (Figure 4.a(i)) is  
358 regular with two minor enlargements between depths 50 - 55 mbgl. The initial tracer concentration  
359 (Figure 4 a(ii)) ranged between 0.85 – 0.99 gL<sup>-1</sup>, with a freshwater front slowly progressing downwards  
360 from the water table reaching >60 mbgl by 2178 minutes.

361 The WTP borehole (Figure 4.b (i)) borehole optical image log shows horizontal and sub-horizontal  
362 feature traces distributed at different depths, coinciding with borehole enlargement on the caliper log  
363 (Figure 4.b (ii)). The borehole diameter is irregular ranging in diameter from 100 and 155 mm, with

364 the diameter enlargements occurring between depths 25 and 37 mbgl. The WTP uniform injection test  
365 (Figure 4.b (iii)) show an initial salt concentration of  $2.75 \text{ gL}^{-1}$  (preserved only near the borehole  
366 bottom and near the water table), with very large distinctive concentration falls (kink points) at 33.5  
367 and 40 mbgl persisting through the test. A freshwater front drives tracer up the borehole from the  
368 kink point at 40 mbgl, with the tracer peak moving progressively upwards to the kink point at 33.5  
369 mbgl. Above 33.5 mbgl tracer dilution is more uniform but less rapid; dilution is relatively slow below  
370 the kink point at 40 mbgl, with little dilution below 42 mbgl.

371 The TP borehole diameter (Figure 4.c(i)) is highly irregular, ranging between 200 and 480 mm, with  
372 diameter enlargement occurring between depths 14.5 and 29 mbgl. The uniform injection (Figure  
373 4.c(ii)) test shows a rapid dilution of tracer, suggesting upward moving freshwater front from the  
374 borehole bottom exiting near the base of the casing at 13 mbgl, reaching 22 mbgl within 20 mins (first  
375 profile; all subsequent profiles show background concentration).

376 The LKF borehole diameter (Figure 4.d (i)) is irregular, ranging from 225 – 460 mm with the majority  
377 of the largest diameters occurring between depths 15m and 26 mbgl. LKF uniform injection data  
378 (Figure 4.d (ii)) show a fairly uniform initial concentration ( $\sim 1.4 \text{ gL}^{-1}$ ) was achieved below 27 mbgl, but  
379 by the time of the first profile (5 – 10 mins) it was slightly lower above this depth ( $\sim 1.0 \text{ gL}^{-1}$  at the  
380 water table), indicating very rapid dilution. Fairly uniform dilution occurred down to around 35 mbgl,  
381 with tracer concentrations approaching background in about 60 mins. Below these depths dilution  
382 was slower.

383 Figure 5 shows selected Pitrak et al. (2007) analyses for the above tests (NB Pitrak plots were prepared  
384 for all depths but only illustrative examples are shown here). Figure 5a and b show linear responses  
385 indicating horizontal crossflow in LKF at depths of 23.5 and 35 mbgl, with some vertical flow influence  
386 at the latter depth due to the relatively better fit at the former depth; Fig. 5c shows a non-linear  
387 response for depth 33.5 mbgl in WTP, indicating that vertical flows contribute to tracer loss at this  
388 depth.

### 389 5.1.2 Point injection tests

390 The results for point injection tests in TP, LKF and WTP boreholes are shown in Figures 6 and 7 (NB  
391 point injecting FHK borehole was not undertaken for logistical reasons). In TP borehole point injection  
392 test at depth 45 mbgl (Figure 6a(ii)), the injected tracer slug moved upwards to the area of enlarged  
393 diameter indicating upwards flow in the borehole, progressively losing tracer mass. [NB tracer mass  
394 for first profile (0-3 mins) of 81 g exceeded injected mass of 75 g, indicating incomplete mixing just  
395 after injection]. Note that no mass was lost between the second and third profiles, ie between depths  
396 38 and 27.5 mbgl, indicating that tracer was conserved in the borehole between these depth.

397 For LKF point injection tests at depths 19.5 and 30 mbgl (monitoring discontinued after 31 min for 30  
398 mbgl injection for logistical reasons) (Figure 6b (ii & iii)) respectively, the profiles show continuous  
399 mass loss with time but little vertical movement of the tracer slugs, confirming the dominance of  
400 lateral horizontal crossflows over vertical flows in the borehole as seen in the uniform injection test  
401 (Figure 4d).

402 Due to the complexity of flowing signatures from uniform injections in WTP borehole (Fig. 4c), three  
403 depths were point injected: 39.5, 33.5, and 41.5 mbgl (Figures 7c – e respectively). In the 39.5 m  
404 injection test (Figure 7c) tracer moves upwards to 34 mbgl progressively losing mass, with no tracer  
405 moving past this depth [the mass from the first profile (1-7 mins) of 84 g again exceeded the injected  
406 mass of 75 g, indicating incomplete mixing within the water column]. In the 33.5 m injection (Figure  
407 7d), the tracer slug moves upwards towards the water table at 25 mbgl, progressively losing mass and  
408 velocity (most of the mass loss occurring immediately below the water table between 27.5 to 25 mbgl).  
409 In the 41.5 m injection (Figure 7e), profiles show little vertical movement of tracer with the peaks  
410 progressively reducing with time, indicating crossflow [mass from first profile (0-4 mins) of 43 g is in  
411 this case less than the 75 g injected].

### 412 5.2 Interpretation

413 5.2.1. Cases showing vertical flows

414 Interpretations of flow patterns for TP and WTP boreholes, which show vertical flows in some sections,  
415 are presented in Figure 8. Figure 8b and e show vertical flow velocities interpolated from the tracer  
416 slug centroid migration rates and tracer slug percentage masses remaining inferred from sequential  
417 profiles shown in Figures 6 and 7. Part c and f show conceptual models of inflows and out-flows from  
418 the boreholes, quantified by sequential application of Equation (7) to each velocity section, in  
419 consonance with caliper logs (Figure 8a and d).

420 For TP borehole (Figure 8c), depths 45 – 38 mbgl show inflow and crossflow, depth interval 38 – 19  
421 mbgl mainly shows upflow, whereas depth interval 19 – 15 mbgl has outflow corresponding to a major  
422 interval of borehole enlargement. Little mass loss and fairly constant upwards velocity between depth  
423 38 – 19 mbgl is suggestive of a zone without inflow or outflow (the small change in vertical velocity  
424 around between 27.5 mbgl and 19 mbgl may reflect diameter enlargement). The average upwards  
425 flow velocity in this current work of  $2.1 \text{ m min}^{-1}$  agrees with average impeller ambient upward flow  
426 speed of  $2 \text{ m min}^{-1}$  from 43 – 15 mbgl, as reported by Parker et al (2019) for TP borehole.

427 For WTP borehole (Figure 8f), the water in the borehole below  $\sim 42 \text{ m bgl}$  is stagnant (see Fig 4c); above  
428 this depth to  $\sim 40 \text{ mbgl}$  (kink in uniform injection profile Fig 4c) the borehole shows inflow and  
429 crossflow, depth interval 39 to 34 mbgl shows upflow with some outflow above 37 mbgl, while the 34  
430 – 33m depth interval shows net inflow (evidenced by the increase upflow velocity above this, Fig 8e).  
431 Upflow velocity begins to fall above  $\sim 30 \text{ m bgl}$  and major tracer mass loss occurs in the depth interval  
432 27.5 – 25 mbgl suggesting progressive outflow corresponding to the major interval of borehole  
433 enlargement immediately below the water table. In contrast Parker et al. (2019) used uniform single  
434 borehole injection test at a time of higher water table, to infer inflows at 40 m and 21 mbgl, with flow  
435 moving upwards and downwards respectively within the borehole to converge at an outflow between  
436 these depths (33.5 mbgl). Comparing the current flow WTP flow model with that from Parker et al  
437 (2019) suggests flow regimes can switch in response to seasonal water table variations {Parker et al

438 (2019) similarly measured larger magnitude borehole flow velocities above 33.5 mbgl than below as  
439 in this study, indicating the most active flow zone is above this depth}.

440 In summary, both the vertical flow cases represent boreholes in valley locations (TP and WTP  
441 boreholes, see Figure 1) showing developed permeability at depth with vertical hydraulic gradients  
442 that drive flow up the borehole, probably resulting from connection to recharge areas of higher  
443 hydraulic heads. The vertical flowrate in the outflow zone of TP is about 2 orders of magnitude  
444 higher than that from WTP probably indicates a larger head difference between intercepted flow  
445 horizons in TP.

#### 446 *5.2.2 Horizontal flow only case*

447 Analysis of data from LKF borehole, which is an example that shows only horizontal cross flow, is  
448 presented in Figure 9. Pitrak et al. (2007) analysis as illustrated in Figure 5 for two selected depths  
449 have been applied to the responses at all depths to produce horizontal specific discharge across the  
450 borehole ( $q_w$ ) at 1.5 m depth intervals (Figure 9b). The calculated discharges are highest within the  
451 zone of water table fluctuation in coincidence with the zone of enhanced diameter in the caliper logs  
452 (Figure 9a), reducing towards the bottom of the borehole, with a marked drop below 35 mbgl. The  
453 results are consistent with solutionally enlarged fractures near the water table, creating the zone of  
454 greatest permeability and flow. In this case, despite the valley location of the borehole, it does not  
455 seem to have intersected any permeability features with higher hydraulic head at depth, hence the  
456 lack of vertical flow in the borehole.

#### 457 *5.2.3 Inference of flowing porosities and groundwater velocities*

458 In this section we explain how the flows detected in the boreholes using the single borehole dilution  
459 approach can potentially be used to infer flowing porosities and groundwater velocities in the aquifer  
460 In order to do this, it is necessary to have hydraulic test data relating to the overall borehole  
461 transmissivity as borehole as an indication of the number and distribution of flowing fractures e.g.

462 from a caliper log interpretation integrated with image and flow logs. In our study, transmissivity was  
463 only available for LKF borehole (8810 m<sup>2</sup>/day) determined in a pumping test (Ward and Williams,  
464 1995), hence, we only applied the workflow to this case. The transmissivity of each 1.5m section  $T_i$   
465 (Figure 9c) was determined by assuming it was proportional to the specific discharge (Figure 9b) for  
466 that section. The number of fractures in each 1.5m section  $N_i$  is annotated on Figure 9c; note this  
467 reduces near the bottom of the borehole.  $T_i$  and  $N_i$  were then used to determine flowing porosity for  
468 each depth interval using equations 8 and 10. Using equation (9), individual fracture transmissivities  
469 ranged between 10–560 m<sup>2</sup>/d (at the bottom and within the water table fluctuation zone respectively  
470 of the borehole. The flowing porosities (Figure 9d) range between  $3.7 \times 10^{-4}$  –  $4.1 \times 10^{-3}$  with an average  
471 of  $2.1 \times 10^{-3}$ , with highest values within the zone of water table fluctuation, coinciding with the largest  
472 caliper enlargements and the lowest values near the borehole base. The average porosity for this work  
473 is similar to the lower end of the range of pumping test-derived flowing porosities for Chalk reported  
474 by Foster and Milton (1974) and Ward and Williams (1995) as  $5 \times 10^{-3}$  –  $1 \times 10^{-1}$  and  $3 \times 10^{-3}$  –  $2.2 \times 10^{-2}$   
475 respectively. In comparison with previous works, this current work also captured the lower porosity  
476 values below the depth of solutional features, whereas pumping tests from the previous works mainly  
477 characterise flowing features within the depth of water table fluctuation.

478 Theoretically, it is possible to use either equation (5) or equation (11) to determine groundwater  
479 velocities within the fractures once the flowing porosity is determined. However, the use of equation  
480 (5) requires a borehole convergence factor  $\alpha$  to be assumed. Borehole convergence factors are often  
481 assumed to be 2 for granular aquifers (Freeze and Cherry, 1979) but are typically much larger for  
482 fractured aquifers, in some cases as high as 7 – 8 (Hall, 1993) or even > 10 (Kearl, 1997). Hence, we  
483 argue that use of equation (5) as previously used by Maldaner et al., (2018) introduces excessive  
484 uncertainty. Here, we instead use equation (11) which requires the horizontal hydraulic gradient in  
485 the aquifer, rather than the convergence factor. In using regional hydraulic gradient, we assume that  
486 groundwater velocities represent far-field velocities and also that the flowing zone is mostly relatively  
487 thin compared to the horizontal flow distances in the borehole-to-borehole tests, so vertical variations

488 in hydraulic gradient may not be important in the analyses. An average hydraulic gradient of  $3.3 \times 10^{-3}$   
489 <sup>3</sup> was used based on historic hydraulic head measurements in the in study catchment (Ward and  
490 Williams, 1995). The inferred horizontal groundwater velocities from the single borehole test range  
491 between  $60 - 850 \text{ md}^{-1}$  (Figure 9e) with the higher values in the zone of enlarged flowing features in  
492 the upper parts of the borehole. These 'single borehole-test' horizontal groundwater velocities are  
493 similar i.e. bound within the upper (thick dashed lines) and lower limits of  $50 - 480 \text{ md}^{-1}$  respectively,  
494 as reported by Ward and William (1995) based on borehole-to-borehole tracer test groundwater  
495 velocities in the Kilham area (see Figure 1 for locations of these tests). There is excellent agreement  
496 between the single borehole-test velocities and borehole-to-borehole tracer tests within the water  
497 table fluctuation zone.

498 This level of agreement suggests that single borehole tests can provide accurate groundwater  
499 velocities despite their difference in scale of investigation from borehole-to-borehole tests (in this  
500 case the injection and detection points in the latter were up to 4.2 km apart). However, the results of  
501 the single-borehole analyses (both for flowing porosity and groundwater velocity) are sensitive to the  
502 identification of flowing fractures. Using caliper log enlargements overestimates the number of  
503 flowing features, since enlargements could represent drilling and flint layer effects rather than  
504 fractures. Secondly, ambient flow may be influenced by different fractures than those that contribute  
505 to transmissivity under pumped conditions Also, fractures within any given interval may have a wide  
506 range of hydraulic apertures rather than a single value as assumed in the use of the Cubic Law.  
507 Nevertheless, the single borehole approach provides a valuable additional low-cost tool for aquifer  
508 characterisation and delineation of groundwater velocities and hence borehole-head protection  
509 zones.

### 510 **5.3 Discussion**

511 The workflow and results obtained in this study have implications for characterisation, groundwater  
512 modelling, and resource management and protection of the specific aquifer investigated, i.e. the



513 Northern Province Chalk, and for similar limestone aquifers, but also for fractured and karstic aquifers  
514 generally. Firstly, preferential flow paths and vertical head gradients need consideration in the  
515 planning and interpretation of groundwater sampling and hydraulic head monitoring. Fast flows  
516 through some sections of the open-section boreholes tested, suggest that purging of such boreholes  
517 during sampling is not a prerequisite for this aquifer as water in these sections is not stagnated.  
518 Secondly, to obtain depth specific samples in boreholes, it would be appropriate to install multi-level  
519 piezometers or else apply straddle packers. However, it is appreciated that such works are expensive,  
520 so where open boreholes are sampled using bailers etc., as is still common practice, employment of  
521 borehole dilution tests beforehand allows appropriate depth selection and interpretation of which  
522 horizons are supplying the sampled water, allowing that seasonal changes may occur. For pumped  
523 samples to be representative of water from the whole borehole, the applied pumping rate needs  
524 should be sufficient (i.e. to exceed the likely borehole vertical flow rates) to sample the full range of  
525 flowing features. Furthermore, groundwater heads measured in open boreholes will represent  
526 transmissivity-weighted composite head in each of the individual horizons connected to the open  
527 borehole. Multi-level piezometers are needed to establish hydraulic head in each separate horizon, in  
528 order to characterise vertical hydraulic gradients. Use of multi-level piezometers installed at selected  
529 depths based on flow logging and potentially, dilution test data also has the advantage that open  
530 boreholes cannot themselves act as potential conduits for contaminants to enter groundwater, or  
531 influence the flow pattern in the aquifer overall.

532 This work has also shown the use of single borehole tests in conjunction with geophysical logs and  
533 hydraulic gradients external to the borehole for inferring borehole and aquifer scale properties. Firstly,  
534 for boreholes dominated by horizontal flows, the use of dilution tests to apportion interval  
535 transmissivity is a cheaper option compared to packer tests (Quinn et al., 2011; Maldaner et al., 2018),  
536 FLUTE profiling (Keller et al., 2013), piezometer installation (Medici et al., 2019) and flow logging (Molz  
537 et al., 1989; Parker et al., 2010). The transmissivity apportionment in this workflow although  
538 developed only for the horizontal flow case, has potential for further development and extension to

539 vertical flow cases. Secondly, although the current work applies the theory of previous works, this is  
540 the first work to use single borehole dilution tests combined with long-interval pumping test data to  
541 rather than slug tests or packer profiling to depth-distribute flowing porosity. Thirdly, using the  
542 determined aquifer parameters for the horizontal flow case, we characterised groundwater velocities  
543 using externally measured hydraulic gradient which compared to other previous works avoided the  
544 assumptions of a flow convergence factor  $\alpha$  and its inherent uncertainties. Our methodology for  
545 determining horizontal groundwater velocities has potential for widespread use on other fractured  
546 aquifers. Finally, although equation (7) has been theorized in other works, this work successfully  
547 implements it to infer inflow, outflow zones and vertical flow for the development and constraining  
548 of borehole scale conceptual models. Note that although we were not able to determine groundwater  
549 velocities from borehole tests showing vertical flow components because of the difficulty in  
550 distributing borehole transmissivity to individual features, the approach could be further developed  
551 for such cases where individual feature transmissivity measurements be available from e.g. packer  
552 tests. Finally, we note that the presence of open borehole sections within aquifers will modify their  
553 natural flow patterns, where these act as conduits for vertical flows. In relatively permeable systems  
554 such as the Chalk, open boreholes will add to natural flow pathways via vertical communicating  
555 features (faults, joints etc) but with overall small effect on the regional flow system. However, such  
556 effects may limit efficacy of the approach in lower permeability systems where such perturbations  
557 may influence regional flow.

558 In the study area, important discrete flow horizons are found throughout the tested depths.. Our data  
559 suggest that these flow features reduce in both frequency and permeability with depth possibly due  
560 to reduced fracture enlargement from slower groundwater circulation or other constrains on the  
561 development of flow features at particular level via karst genesis (Allen et al., 1997; Ford and Williams,  
562 2007).. This is expected for the Chalk as seen in previous works (Williams et al., 2006; Maurice et al.,  
563 2010; Farrant et al., 2016; Parker et al., 2019). The vertical distribution of flow horizons in boreholes  
564 together with the dilution test results imply that the bulk of formation effective porosity and borehole

565 transmissivity lies within the zone of water table fluctuation, indicating that resource assessment and  
566 valuation must be done in conjunction with a consideration for seasonality and using geophysical logs.  
567 The flow regime change observed in WTP borehole in response to seasonal hydraulic head variations  
568 is important not only for the Chalk, but other unconfined fractured aquifers with respect to  
569 contaminant monitoring and aquifer remediation.

570 The results of this work (low effective porosities, flow at discrete horizons, fast groundwater velocities)  
571 and previous tracer test results are typical of a karstic aquifer, implying that the Chalk is vulnerable to  
572 pollution as contaminants have short travel times from recharge areas to boreholes. The findings also  
573 have implication for conceptual solute transport model development for the purpose of well-head  
574 protection. Modelling aquifers such as Chalk with preferential flowpaths can be fraught with  
575 uncertainties. We recommend using a multiple conceptual model approach and systematically  
576 collecting data to test and constrain transport models (Brassington and Younger, 2010; Worthington,  
577 2015; Bredehoeft, 2005). In this type of aquifer, it is essential that models purporting to simulate both  
578 available resource and solute transport correctly incorporate seasonality, given the dominant nature  
579 of the (often rather thin) zone of solutionally enhanced permeability in the zone of water table  
580 fluctuation.

581 The implementation of our workflow shows the potential for open-borehole dilution tests in reducing  
582 costs of hydrogeological investigations at both the borehole and catchment scale, for aquifer  
583 characterisation, prediction of horizontal groundwater velocities and development of sound  
584 conceptual models. This relatively cheap workflow is potentially applicable for the characterisation of  
585 other fractured aquifers.

## 586 **6. Conclusion**

587 Knowledge of preferential flowpaths and vertical head gradients are important for characterising  
588 groundwater in fractured aquifers like the Cretaceous Chalk. However, because of their heterogenous  
589 and anisotropic nature, detailed characterisation of such aquifers is needed for adequate modelling

590 of both resource and pollution vulnerability. Borehole-to-borehole 'catchment' scale tracer tests are  
591 one effective way of characterising such aquifers but are time consuming and expensive to perform.  
592 Single borehole dilution tests are cheaper to perform, their results have previously been considered  
593 more difficult to interpret. In this study, we propose a new workflow for ambient flow single borehole  
594 dilution tests showing that where interpreted in conjunction with other data, they can be effectively  
595 used to characterise and constrain flowing features in fractured and karstic aquifers, and that their  
596 results are consistent with those from other more expensive approaches.

597 In the study reported here of the unconfined Cretaceous Chalk aquifer of East Yorkshire, UK, single  
598 borehole dilution tests were used to identify flowing features in monitoring boreholes with long open  
599 sections, from the dilution pattern shown by the injected tracer due to inflowing formation water  
600 under natural (ambient) flow conditions. Both uniform injection (tracer distributed over whole section  
601 of the borehole that is open to the aquifer) and point injection tracer test (discrete slug of tracer  
602 injected at a single depth) were performed. The tracer tests were initially qualitatively interpreted via  
603 signature methods to distinguish between boreholes dominated by vertical and horizontal flows.  
604 Then, for the case of boreholes dominated by horizontal flow, test data were interpreted in  
605 combination with long-interval pumping test data transmissivity and geophysical logs to yield fracture  
606 kinematic porosity versus depth. Flowing porosities ranged between  $3.7 \times 10^{-4}$  –  $4.1 \times 10^{-3}$ , in good  
607 agreement with those found using other methods. Combining with external hydraulic gradient, these  
608 data yielded depth distributed horizontal groundwater velocities of  $60 - 850 \text{ md}^{-1}$ , which closely  
609 agreed with those from borehole-to-borehole tracer tests ( $50 - 480 \text{ md}^{-1}$ ) reported in previous studies  
610 of the same catchment. [Note that the use of external hydraulic gradients for the derivation of  
611 horizontal groundwater velocities proposed here circumvents many uncertainties associated with  
612 previous interpretational approaches for single borehole data.] For boreholes showing vertical flow,  
613 both uniform and point injection tracer test data were interpreted in conjunction with geophysical  
614 logs to yield in-borehole vertical flow velocities, and hence characterise borehole inflows, crossflows  
615 and outflows. Vertical velocities inferred from the borehole dilution tests broadly agreed with those

616 measured using flow logging tests conducted in previous work in the same boreholes. The identified  
617 flowing features were used to infer conceptual flow models, enabling an improved understanding of  
618 catchment-scale aquifer heterogeneities.

619 The findings from this work show that long-interval single borehole dilution tests represent a low cost  
620 but effective hydrogeological tool for the characterisation of fractured and karstic aquifers. They can  
621 be employed on open boreholes in consolidated fractured aquifers in order to target depths for  
622 sampling, further hydraulic testing, or piezometer installation. Combining uniform and point injection  
623 approaches allows verification of the interpretational approaches applied; point injection tests are  
624 particularly relevant where vertical flows occur within boreholes. For horizontal flow conditions,  
625 dilution test data can be used to distribute transmissivity from long-interval hydraulic tests,  
626 characterise fracture aperture and porosity, and in combination with externally-measured hydraulic  
627 gradients to infer groundwater velocities in the formation.

628

## 629 **Acknowledgements**

630 We thank Kirk Handley from the School of Earth and Environment for assisting in fieldwork. We also  
631 thank Dr Louise Maurice of the British Geological Survey for field kit support and guidance, and Rolf  
632 Farrell and Edward Wrathmell from the Environment Agency of England and Wales for input at the  
633 early stages of this work. We also thank two anonymous reviewers for their review comments.

## 634 **Funding information**

635 This work was made possible by: Scholarship Award No. GHCS – 2015- 147 from the joint sponsorship  
636 of the Commonwealth Scholarship Commission (CSC) UK and University of Leeds; Fieldwork Support  
637 Grant and data licensing from the UK Environment Agency.

## 638 **References**

639 Akoachere, R.A.I.I. and Van Tonder, G. 2009. Two new methods for the determination of hydraulic

640 fracture apertures in fractured-rock aquifers. *Water SA*. **35**(3),pp.349–360.

641 Allen, D.J., Brewerton, L.J., Coleby, L.M., Gibbs, B.R., Lewis, M.A., MacDonald, A.M., Wagstaff, S.J.  
642 and Williams, A.T. 1997. *The physical properties of major aquifers in England and Wales*. British  
643 *Geological Survey Technical Report WD/97/34*. Environment Agency R&D Publication 8. British  
644 Geological Survey Technical Report WD/97/34.

645 Bloomfield, J. 1996. Characterisation of hydrogeologically significant fracture distributions in the  
646 Chalk: An example from the Upper Chalk of southern England. *Journal of Hydrology*. **184**(3–  
647 4),pp.355–379.

648 Bottrell, S.H., Thornton, S.F., Spence, M.J., Allshorn, S. and Spence, K.H. 2010. Assessment of the use  
649 of fluorescent tracers in a contaminated Chalk aquifer. *Quarterly Journal of Engineering  
650 Geology and Hydrogeology*. **43**(2),pp.195–206.

651 Boulding, J. 1993. *Subsurface Characterization and Monitoring Techniques. A Desk Reference Guide.  
652 Volume I: Solids and Ground Water Appendices A and B*. EPA/625/R-93/003a. Washington, DC.

653 Brainerd, R.J. and Robbins, G.A. 2004. A tracer dilution method for fracture characterization in  
654 bedrock wells. *Ground water*. **42**(5),pp.774–780.

655 Brassington, F.C. 1992. Measurements of Head Variations within Observation Boreholes and their  
656 Implications for Groundwater Monitoring. *Water and Environment Journal*. **6**(3),pp.91–100.

657 Brassington, F.C. and Younger, P.L. 2010. A proposed framework for hydrogeological conceptual  
658 modelling. *Water and Environment Journal*. **24**(4),pp.261–273.

659 Bredehoeft, J. 2005. The conceptualization model problem — surprise. *Hydrogeology Journal*.  
660 **13**,pp.37–46.

661 Buckley, D.K. and Talbot, J.C. 1994. *Interpretation of geophysical logs of the Kilham area, Yorkshire  
662 Wolds, to support groundwater tracer studies*. British Geological Survey Technical

663 Report,WD/94/10C.

664 Cook, P.G. 2003. *A guide to regional groundwater flow in fractured rock aquifers*. South Australia:  
665 CSIROSeaview Press.

666 Dalton, M.G., Huntsman, B.E. and Bradbury, K. 2006. Acquisition and interpretation of water level  
667 data *In*: D. Nielsen and G. L. Nielsen, eds. *The essential handbook of ground-water sampling*.  
668 Boca Raton, Florida: CRC Press, p. 309.

669 Datel, J. V., Kobr, M. and Prochazka, M. 2009. Well logging methods in groundwater surveys of  
670 complicated aquifer systems: Bohemian Cretaceous Basin. *Environmental Geology*.  
671 **57**(5),pp.1021–1034.

672 Day-Lewis, F.D., Johnson, C.D., Paillet, F.L. and Halford, K.J. 2011. A Computer Program for Flow-Log  
673 Analysis of Single Holes (FLASH). *Ground Water*. **49**(6),pp.926–931.

674 Doughty, C., Takeuchi, S., Amano, K., Shimo, M. and Tsang, C.-F. 2005. Application of multirate  
675 flowing fluid electric conductivity logging method to well DH-2, Tono Site, Japan. *Water*  
676 *Resources Research*. **41**(10),pp.1–16.

677 Doughty, C., Tsang, C.-F., Hatanaka, K., Yabuuchi, S. and Kurikami, H. 2008. Application of direct-  
678 fitting, mass integral, and multirate methods to analysis of flowing fluid electric conductivity  
679 logs from Horonobe, Japan. *Water Resources Research*. **44**(8),pp.1–19.

680 Doughty, C. and Tsang, C. 2005. Signatures in flowing fluid electric conductivity logs. *Journal of*  
681 *Hydrology*. **310**,pp.157–180.

682 Downing, R.A. 1998. *Groundwater - our hidden asset*. Produced by the UK Groundwater Forum.  
683 Published by the British Geological Survey.

684 Drost, W., Klotz, D., Koch, A., Moser, H., Neumaier, F. and Rauert, W. 1968. Point dilution methods of  
685 investigating ground water flow by means of radioisotopes. *Water Resources Research*.

686           **4(1)**,pp.125–146.

687   Edmunds, W.M., Buckley, D.K., Darling, W.G., Milne, C.J., Smedley, P.L. and Williams, A.T. 2001.

688           Palaeowaters in the aquifers of the coastal regions of southern and eastern England. *Geological*

689           *Society, London, Special Publications. 189(1)*,pp.71–92.

690   Farrant, A.R., Woods, M.A., Maurice, L., Haslam, R., Raines, M. and Kendall, R. 2016. *Geology of the*

691           *Kilham area and its influence on groundwater flow. British Geological Survey Commissioned*

692           *Report CR/16/023.*

693   Ford, D. and Williams, P. 2007. *Karst Hydrogeology and Geomorphology*. Chichester: Wiley.

694   Foster, S.S.D. and Milton, V.A. 1976. *Hydrogeological basis for large-scale development of*

695           *groundwater storage capacity in the East Yorkshire Chalk*. Report of the Institute of Geological

696           Sciences, 76/7.

697   Foster, S.S.D. and Milton, V.A. 1974. The permeability and storage of an unconfined chalk aquifer.

698           *Hydrological Sciences Bulletin. XIX(4)*,pp.485–500.

699   Freeze, R.A. and Witherspoon, P.A. 1968. Theoretical Analysis of Regional Ground Water Flow 3.

700           Quantitative Interpretions. *Water Resources Research. 4(3)*,pp.581–590.

701   Gale, I.N. and Rutter, H.K. 2006. *The Chalk aquifer of Yorkshire*. British Geological Survey Research

702           Report. RR/06/04.

703   Gustafsson, E. and Anderson, P. 1991. Groundwater flow conditions in a low-angle fracture zone at

704           Finnsjon, Sweden. *Journal of Hydrology. 126*,pp.79–111.

705   Hall, S.H. 1993. Single Well Tracer Tests in Aquifer Characterization. *Groundwater Monitoring &*

706           *Remediation. 13(2)*,pp.118–124.

707   Jones, H., Gale, I., Barker, J. and Shearer, T. 1993. *Hydrogeological report on the test pumping of*

708           *Hutton Cranswick, Kilham, and Elmswell boreholes. British Geological Survey Technical Report,*



709 WD/93/9.

710 Kearn, P. 1997. Observations of particle movement in a monitoring well using the colloidal  
711 borescope. *Journal of Hydrology*. **200**,pp.323–344.

712 Keller, C.E., Cherry, J.A. and Parker, B.L. 2013. New method for continuous transmissivity profiling in  
713 fractured rock. *Groundwater*. **52**(3),pp.352–367.

714 Keys, W.S. 1990. *Chapter E2. Borehole geophysics applied to ground-water investigations.*  
715 *Techniques of Water-Resources Investigations of the United States Geological Survey*. United  
716 States Geological Survey.

717 Knapp, M.F. 2005. Diffuse pollution threats to groundwater: A UK water company perspective.  
718 *Quarterly Journal of Engineering Geology and Hydrogeology*. **38**(1),pp.39–51.

719 Kobr, M. 2003. Geophysical techniques applied to aquifer hydrodynamics. *Bollettino di Geofisica*  
720 *Teorica ed Applicata*. **44**(3–4),pp.307–319.

721 Lewis, D.C., Kriz, G.J. and Burgy, R.H. 1966. Tracer dilution sampling technique to determine  
722 hydraulic conductivity of fractured rock. *Water Resources Research*. **2**(3),pp.533–542.

723 Liang, X., Liu, Y., Jin, M., Lu, X. and Zhang, R. 2010. Direct observation of complex Tothian  
724 groundwater flow systems in the laboratory. *Hydrological Processes*. **3573**,pp.3568–3573.

725 Maldaner, C.H., Quinn, P.M., Cherry, J.A. and Parker, B.L. 2018. Improving estimates of groundwater  
726 velocity in a fractured rock borehole using hydraulic and tracer dilution methods. *Journal of*  
727 *Contaminant Hydrology*. [Online]. **214**(May),pp.75–86. Available from:  
728 <https://doi.org/10.1016/j.jconhyd.2018.05.003>.

729 Maurice, L., Barker, J.A., Atkinson, T.C., Williams, A.T. and Smart, P.L. 2010. A Tracer Methodology  
730 for Identifying Ambient Flows in Boreholes. *Ground Water*. **49**(2),pp.227–238.

731 McMillan, L.A., Rivett, M.O., Tellam, J.H., Dumble, P. and Sharp, H. 2014. Influence of vertical flows

732 in wells on groundwater sampling. *Journal of Contaminant Hydrology*. [Online]. **169**,pp.50–61.  
733 Available from: <http://dx.doi.org/10.1016/j.jconhyd.2014.05.005>.

734 Medici, G., West, L. and Banwart, S. 2019. Groundwater flow velocities in a fractured carbonate  
735 aquifer-type : Implications for contaminant transport. *Journal of Contaminant Hydrology*.  
736 [Online]. **222**,pp.1–16. Available from: <https://doi.org/10.1016/j.jconhyd.2019.02.001>.

737 Moir, R.S., Parker, A.H. and Bown, R.T. 2014. A simple inverse method for the interpretation of  
738 pumped flowing fluid electrical conductivity logs. *Water Resources Research*. (50),pp.6466–  
739 6478.

740 Molz, F.J., Morin, R.H., A.E., H., Melville, J.G. and Guven, O. 1989. The Impeller Meter for Measuring  
741 Aquifer Permeability Variations: Evaluation and Comparison with Other Tests. *Water Resources*  
742 *Research*. **25**(7),pp.1677–1683.

743 Novakowski, K., Bickerton, G., Lapcevic, P., Voralek, J. and Ross, N. 2006. Measurements of  
744 groundwater velocity in discrete rock fractures. *Journal of Contaminant Hydrology*. **82**(1–  
745 2),pp.44–60.

746 Novakowski, K.S., Lapcevic, P.A., Voralek, J. and Bickerton, G. 1995. Preliminary interpretation of  
747 tracer experiments conducted in a discrete rock fracture under condition of natural flow.  
748 *Geophysical Research Letters*. **22**(11),pp.1417–1420.

749 Paillet, F.L. 1991. Use of geophysical well logs in evaluating crystalline rocks for siting of radioactive  
750 waste repositories. *The Log Analyst*. **32**(2),pp.85–107.

751 Paillet, F.L. and Pedler, W.H. 1996. Integrated borehole logging methods for wellhead protection  
752 applications. *Engineering Geology*. **42**(2–3),pp.155–165.

753 Paillet, F.L., Williams, J.H., Urik, J., Lukes, J., Kobr, M. and Mares, S. 2012. Cross-borehole flow  
754 analysis to characterize fracture connections in the Melechov Granite, Bohemian-Moravian  
755 Highland, Czech Republic. *Hydrogeology Journal*. **20**(1),pp.143–154.

756 Parker, A.H., West, L.J. and Odling, N.E. 2019. Well flow and dilution measurements for  
757 characterization of vertical hydraulic conductivity structure of a carbonate aquifer. *Quarterly*  
758 *Journal of Engineering Geology and Hydrogeology*. [Online]. **52**(1),pp.74–82. Available from:  
759 <https://doi.org/10.1144/qjegh2016-145>.

760 Parker, A.H., West, L.J., Odling, N.E. and Bown, R.T. 2010. A forward modeling approach for  
761 interpreting impeller flow logs. *Ground Water*. **48**(1),pp.79–91.

762 Pedler, W.H., Barvenik, C.F., Tsang, C.F. and Hale, F.V. 1990. Determination of Bedrock Hydraulic  
763 Conductivity and Hydrochemistry Using a Wellbore Fluid Logging Method *In: Proceedings of the*  
764 *Fourth National Outdoor Action Conference on Aquifer Restoration, Ground Water Monitoring*  
765 *and Geophysical Methods, Las Vegas, Nevada, Dublin, Ohio: National Well Water Association.,*  
766 pp. 39–53.

767 Pedler, W.H., Head, C.L. and Williams, L.H. 1992. Hydrophysical Logging: A New Wellbore Technology  
768 for Hydrogeologic and Contaminant Characterization of Aquifers *In: Proceedings of the Sixth*  
769 *National Outdoor Action Conference on Aquifer Restoration, Ground Water Monitoring and*  
770 *Geophysical Methods, Las Vegas, Nevada, Dublin, Ohio: National Well Water Association.,* pp.  
771 701–715.

772 Piccinini, L., Fabbri, P. and Pola, M. 2016. Point dilution tests to calculate groundwater velocity: an  
773 example in a porous aquifer in northeast Italy. *Hydrological Sciences Journal*. [Online].  
774 **61**(8),pp.1512–1523. Available from: <http://dx.doi.org/10.1080/02626667.2015.1036756>.

775 Pitrak, M., Mares, S. and Kobr, M. 2007. A simple borehole dilution technique in measuring  
776 horizontal ground water flow. *Ground Water*. **45**(1),pp.89–92.

777 Price, M. 1987. Fluid flow in the Chalk of England *In: J. C. Goff and B. P. J. Williams, eds. FluidFlow in*  
778 *Sedimentary Basins and Aquifers*. Geological Society Special Publication, pp. 141–156.

779 Price, M., Low, R.G. and McCann, C. 2000. Mechanisms of water storage and flow in the unsaturated

780 zone of the Chalk aquifer. *Journal of Hydrology*. **233**(1–4),pp.54–71.

781 Qian, J., Chen, Z., Zhan, H. and Guan, H. 2011. Experimental study of the effect of roughness and  
782 Reynolds number on fluid flow in rough-walled single fractures : a check of local cubic law.  
783 *Hydrological Processes*. **622**,pp.614–622.

784 Quinn, P.M., Parker, B.L. and Cherry, J.A. 2011. Using constant head step tests to determine  
785 hydraulic apertures in fractured rock. *Journal of Contaminant Hydrology*. **126**(1–2),pp.85–99.

786 Saines, M. 1981. Errors in the interpretation of groundwater level data. *Groundwater Monitoring  
787 and Remediation, Spring Issue.*,pp.56–51.

788 Shuter, E. and Teasdale, W.E. 1989. *Application of Drilling, Coring and Sampling Techniques to Test  
789 Holes and Wells. Techniques of Water-Resource Investigations of the United States Geological  
790 Survey. Book 2. Ch. F1.*

791 Singhal, B.B.S. and Gupta, R.P. 1999. *Applied Hydrogeology of Fractured Rocks*. Boston: Kluwer  
792 Academic Publishers.

793 Smedley, P., Neumann, I. and Farrell, R. 2004. *Baseline Report Series: 10. The Chalk Aquifer of  
794 Yorkshire and North Humberside*. British Geological Survey and UK Environment Agency.

795 Snow, D.T. 1969. Anisotropic Permeability of Fractured Media. *Water Resources Research*.  
796 **5**(6),pp.1273–1288.

797 van Tonder, G., Riemann, K. and Dennis, I. 2002. Interpretation of single-well tracer tests using  
798 fractional-flow dimensions. Part 1: Theory and mathematical models. *Hydrogeology Journal*.  
799 **10**,pp.351–356.

800 Toth, J. 1962. A Theory of Groundwater Motion in Small Drainage Basins Hydrology in Central  
801 Alberta, Canada. *Journal of Geophysical Research*. **67**(11),pp.4375–4387.

802 Toth, J. 2009. *Gravitational Systems of Groundwater Flow: Theory, Evaluation, Utilization*.

803 Cambridge: Cambridge University Press.

804 Tsang, C.-F. and Doughty, C. 2003. Multirate flowing fluid electric conductivity logging method.  
805 *Water Resources Research*. **39**(12),p.SBH 12-1-8.

806 Tsang, C., Hufschmied, P. and Hale, F.V. 1990. Determination of Fracture Inflow Parameters With a  
807 Borehole Fluid Conductivity Logging Method. *Water Resources Research*. **26**(4),pp.561–578.

808 Ward, R., Fletcher, S., Ever, S. and Chadha, S. 2000. Tracer testing as an aid to groundwater  
809 protection *In: Tracers and Modelling in Hydrogeology*. Liege, Belgium: IAHR, pp. 85–90.

810 Ward, R., Williams, A., Barker, J., Brewerton, L. and Gale, I. 1998. *Groundwater Tracer Tests : a*  
811 *review and guidelines for their use in British aquifers*. British Geological Survey Technical  
812 Report, WD/98/19, Environment Agency R&D Technical Report W160.

813 Ward, R.S., Chadha, D.S., Aldrick, J. and Brewerton, L.J. 1998. *A Tracer Investigation of Groundwater*  
814 *Protection Zones around Kilham PWS Well, East Yorkshire*. British Geological Survey Report  
815 *WE/98/19*.

816 Ward, R.S. and Williams, A.T. 1995. *A tracer test in the Chalk near Kilham, North Yorkshire*. British  
817 *Geological Survey Report WD/95/7*.

818 Waters, A. and Banks, D. 1997. The chalk as a karstified aquifer: closed circuit television images of  
819 macrobiota. *Quarterly Journal of Engineering Geology*. **30**,pp.143–146.

820 Weight, W.D. 2008. *Hydrogeology Field manual* 2nd ed. New York: Mc-Graw Hill.

821 West, L.J. and Odling, N.E. 2007. Characterization of a multilayer aquifer using open well dilution  
822 tests. *Ground Water*. **45**(1),pp.74–84.

823 Williams, A., Bloomfield, J., Griffiths, K. and Butler, A. 2006. Characterising the vertical variations in  
824 hydraulic conductivity within the Chalk aquifer. *Journal of Hydrology*. **330**(1–2),pp.53–62.

825 Witherspoon, P.A., Wang, J.S.Y., Iwai, K. and Gale, J.E. 1980. Validity of Cubic Law for Fluid Flow in a

826 Deformable Rock Fracture. *Water Resources Research*. **16**(6),pp.1016–1024.

827 Worthington, S.R.H. 2015. Diagnostic tests for conceptualizing transport in bedrock aquifers. *Journal*  
828 *of Hydrology*. [Online]. **529**,pp.365–372. Available from:  
829 <http://dx.doi.org/10.1016/j.jhydrol.2015.08.002>.

830 Xu, Y., van Tonder, G.J., van Wyk, B., van Wyk, E. and Aleobua, B. 1997. Borehole dilution experiment  
831 in a Karoo aquifer in Bloemfontein. *Water SA*. **23**(2),pp.141–145.

832 Zemanek, J.O.E., Gleen, E.E., Norton, L.J. and Caldwell, R.L. 1970. Formation Evaluation by Inspection  
833 with the Borehole Televiewer. *Geophysics*. **35**(2),pp.254–269.

834

835

836

837

838

839

840

841

842

843

844

845

846

847

848

849

850

851 **Paper figure labels**

852 **Figure 1:** Study area: (a) Inset map of Great Britain and location of study area; (b) Single-  
853 borehole dilution test boreholes (red squares) with their elevation above ordnance datum  
854 superimposed on geology of study area, LKF BH: Little Kilham Farm Borehole, 39.96 mAoD;  
855 TP BH: Tancred Pit Borehole, 36.40 mAoD; FHK BH: Field House Farm, Kilham Borehole,  
856 94.42 mAoD; WTP: Weaverthorpe Borehole, 70.00 mAoD. Black circles and arrows for  
857 borehole-to-borehole connectivity and resultant groundwater velocities between boreholes  
858 (HPT BH: Henpit Hole Borehole, 48.86 mAoD; MD BH: Middledale Borehole, 43.72 mAoD;  
859 LKF). © Crown Copyright & Database Right 2019. Ordnance Survey (Digimap Licence).  
860 Geological Map Data BGS © UKRI 2019.

861 **Figure 2:** Experimental set up: (a) Uniform open-borehole dilution test; (b) Point injection test.

862 **Figure 3:** Work flow and decision tree for analysing single-borehole dilution tests.

863 **Figure 4:** Example single borehole uniform test results: (a) FHK caliper and uniform injection  
864 (09/08/2017); (b) WTP borehole image log, caliper (Butcher and Townsend, 2017) and uniform  
865 injection (03/08/2017); (c) TP caliper and uniform injection (13/05/2016); (d) LKF caliper and  
866 uniform injection (20/07/2017).

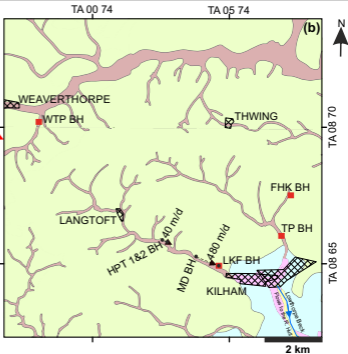
867 **Figure 5:** Horizontal flow model regression plot for: (a) LKF depth 23.5 mbgl; (b) LKF depth  
868 35 mbgl; (c) WTP depth 33.5 mbgl. Note axes scales vary.

869 **Figure 6:** TP (28/06/2016) and LKF (24/11/2017) single borehole point dilution test: (a) TP  
870 caliper and injection results for depth 45 mbgl; (b) LKF caliper log and injection results for  
871 depth: (ii) 19.5 mbgl; (iii) 30 mbgl.



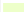




872 **Figure 7:** WTP single borehole point injection test results (24/11/2017) (red arrows indicate  
873 depth of injection). (a) borehole optical image log (red dashed lines mark probable flowing  
874 features); (b) caliper log; (c), (d), (e) at: (c) 39.5; 33.5; and 41.5 mbgl respectively. (NB: The  
875 salinity peak in the bottom section of WTP is the remnant of NaCl left from the previous uniform  
876 injection test).

877 **Figure 8:** Vertical flow cases interpretation. (a) TP caliper log; (b) TP vertical velocity and  
878 mass plot (red dashed line) with depth (75 g injection depth 45 m bgl); (c) TP flow model; (d)  
879 WTP caliper log; (e) WTP velocity and mass plot (red dashed lines) with depth (75 g injection  
880 at depths 39.5 and 33.5 mbgl; (f) WTP flow model.

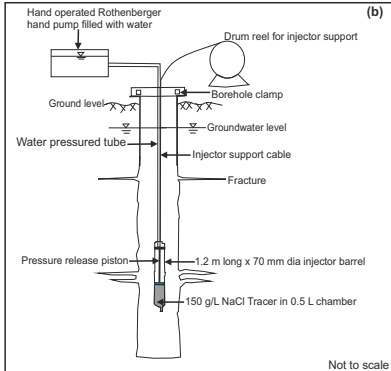
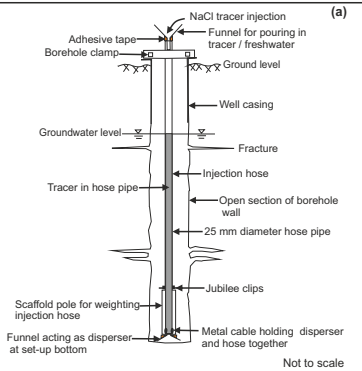
881 **Figure 9:** Interpretation for LKF HP horizontal flow case: (a) caliper log; (b) specific discharge  
882 in borehole,  $q_w$  with depth; (c) dilution apportioned transmissivity ( $T_i$ ), with annotations of  
883 number of flowing features ( $N_i$ ) inferred from caliper diameter enlargements in each 1.5 m  
884 depth interval (d) porosity variation with depth from cubic law; (e) horizontal groundwater  
885 velocities versus depth from single borehole tests compared with upper and lower limits from  
886 borehole-to-borehole tracer tests indicated in Figure 1 (dashed lines).

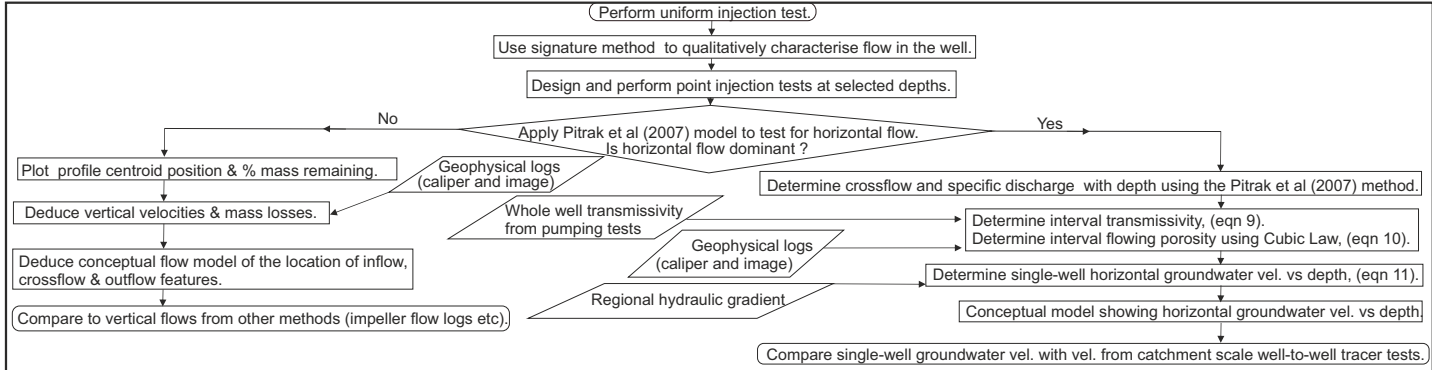


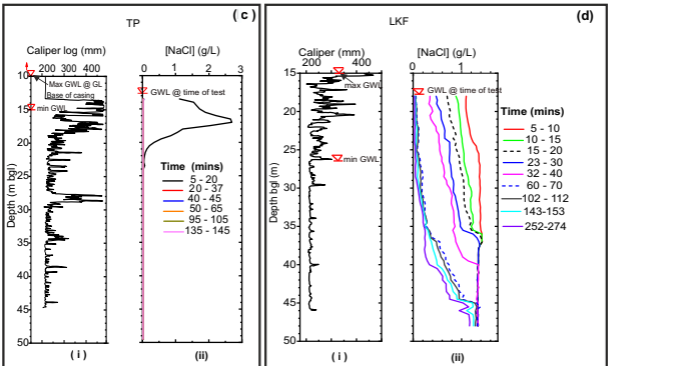
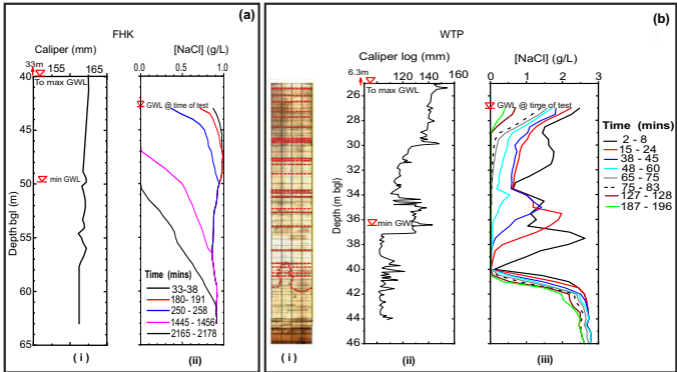
**Map Legend**

-  Towns
-  Surface water features
- Bedrock Geology**
-  Cretaceous Chalk
- Superficial deposits**
-  Alluvium
-  Glaciofluvial deposits
-  Devensian till
-  River terrace deposits

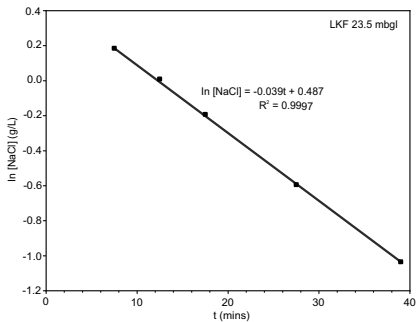




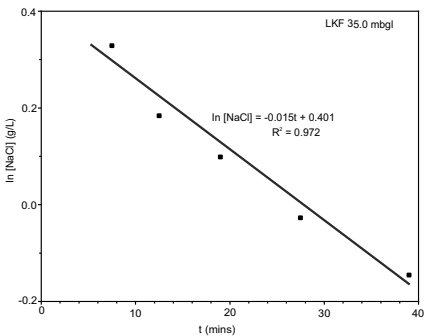




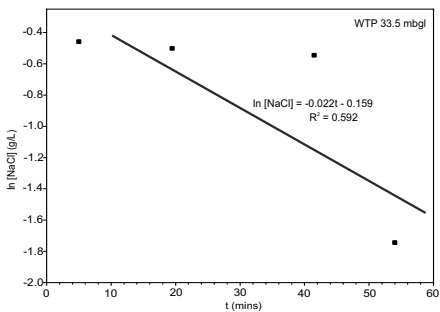
(a)



(b)

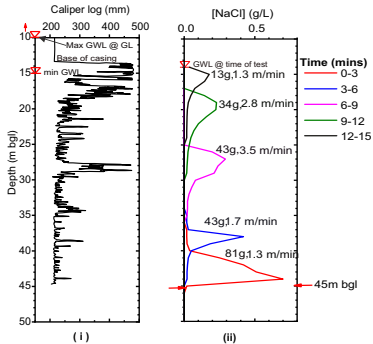


(c)

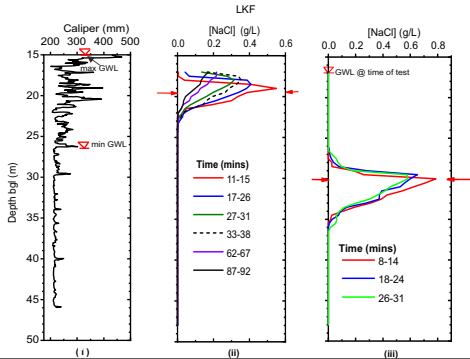


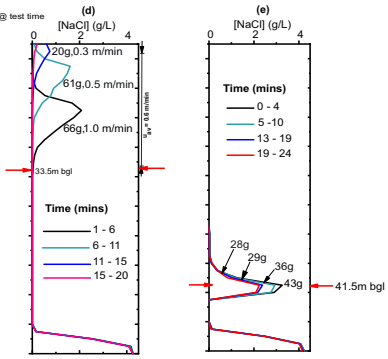
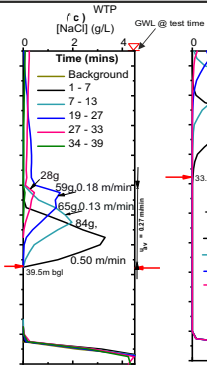
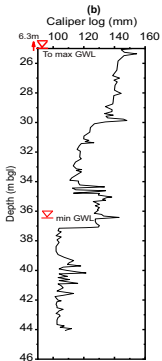
TP

(a)



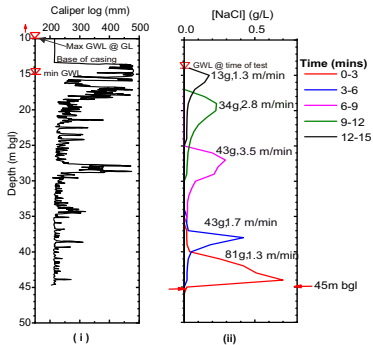
(b)



**(a)**

TP

(a)



(b)

